DINAME 2019 - Proceedings of the XVIII International Symposium on Dynamic Problems of Mechanics,
M.A. Savi, T.G. Ritto and W.M. Bessa (Editors), ABCM, Buzios, RJ, Brazil, March 10th to 15th, 2019

On the evaluation of band gaps created by FDM printed unit cell with piezo disks

Rodrigues, Gabriel K.[1]**, de Oliveira, Leopoldo P. R.**[1]

[1] Escola de Engenharia de São Carlos, Universidade de São Paulo, Av. Trabalhador São-Carlense, 400, 13565-090 São Carlos – SP, Brasil, gabriel.konda.rodrigues@usp.br

Abstract: Research in metamaterials gains an ever-increasing interest in the field of noise and vibration control. The ability of creating band gap zones without penalizing other parameters is the main purpose, and goal, of this kind of solution. More recently, researches are also exploring the addition of smart materials, such as piezoelectric patches, on the metamaterials for the improvement of the band gap zone, such as broadening the gap or by making more robust with a deeper valley. These techniques often exploit the usage of some passive circuitry, such a LC shunt, or even going more sophisticated with Digital Signal Processing for active control approaches. However, the band gap border peaks that arise from exploiting local resonant metamaterials are mostly neglected on these studies. In this paper we analyze the mechanical behavior of beam-like structure coupled with periodic unit cells obtained by FDM printing with a piezo disk embedded connected with passive circuitry (LC shunt circuit). Some insights about the modelling parameters of the cells lattice as well as the discussion about the variation of piezoelectric proprieties, such as electromechanical coupling, and their impact on the full smart metastructure behavior are shown. A novel means of addressing the border peaks is also presented. The results section shows the possibility to nullify the border peaks with the piezo disks resulting in a stop band without the penalty of side peaks.

Keywords: metamaterial, periodic structure, smart material

LIST OF SYMBOLS

m – Elementary mass

c – Elementary damping

k – Elementary Stiffness

l – Length

x – Coordinate displacement

$_r$ – At resonator

$_s$ – At host structure

v – Electric tension

w – lateral beam displacement

A_C – internal capacitance gain

A_θ – electromechanical gain

C_p – internal piezo capacitance

S – Cross section area

T – Kinect Energy

U – Internal Energy

θ – electromechanical coupling factor

μ – Mass ratio

ω – Normalized frequency

ρ – Density

INTRODUCTION

Metamaterials poses as an interesting research field on noise and vibration control (Essink; Inman, 2016; Miranda Júnior; Ferreira; Dos Santos, 2017; Yang; Lee; Kim, 2016). Based on the proprieties of photonics crystals for creating a band gap by the Bragg scattering mechanism, in which the phononic crystals also rely, Liu et al.(2000) achieved the first mechanic metamaterial. As this solution has the ability of creating band gap zones without penalizing other structural parameters, the research field have grown in interest in the last two decades.

Later, sub-Bragg wavelength band gap mechanisms were proposed based on locally resonant (LR) structures and wave manipulation as lensing, bending and cloaking (Cummer; Christensen; Alù, 2016; Huang; Shen; Jing, 2016). In addition, piezoelectric patches grew in relevance for its capability of creating those effects without penalizing other structural parameters opening possibilities for tunable control systems (Nouh; Aldraihem; Baz, 2016; Zhang et al., 2015) . When dealing with subwavelength LR metamaterials, the structural design of each cell can be intricate which, together with the necessity of manufacturing enough cells for assembling the full lattice structure, often leads to additive manufacturing (Bilal; Foehr; Daraio, 2017; Qureshi; Li; Tan, 2016). These techniques are, on their own, also gaining interest in many engineering areas, from material sciences and manufacturing, to those related to the performance assessment of such 3D printed parts.

Among others, the Fused Deposition Modeling (FDM) is interesting for its capability of creating somehow complex geometries (Schumacher et al., 2015) at a relatively low cost (Bosqué, 2015). In this way, as far as the design of FDM manufactured metamaterials is concerned, the understanding of the parameters on the behavior of such structures is one of the key steps on the development of a metamaterial (sub)structure. In addition, the usage of piezo disks brings the discussion of electromechanical couple and circuitry performance in vibration attenuation.

The addition of the piezoelectric effect to a unit cell opens the possibilities for an active-passive solution with the exploitation of inverse effect as well as a full robust passive solution by the direct effect. Both of those solutions are bounded by the electromechanical coupling factor θ, which depends on a material propriety, but also is heavily influenced by geometric considerations. Bonded with the coupling factor, the internal capacitance of the piezo patch, C_p, is heavily dependent of those same attributes. Therefore, this work tries to evaluate qualitatively the influence of such parameters on the full smart metastructure as well as some discussion about the modelling of the unit cell system considering a FDM printed structure.

METAMATERIAL STRUCTURE MODEL

The unit cell concept is often used for the metamaterial analysis (Claeys et al., 2016; Li; Zhang; Liu, 2017; Raghavan; Phani, 2013) as the full lattice is composed by a periodic arrangement of these cells. Therefore, the modelling of these cells is a key point for the analysis of the metastructure. For to achieve the dynamic behavior of the cell is very common the usage of lumped mass model, either for purely mechanical or mix type (e.g. electromechanical) (Hu et al., 2016; Sugino et al., 2016). Considering a lumped system with a piezo, see in Fig. 1, one can write:

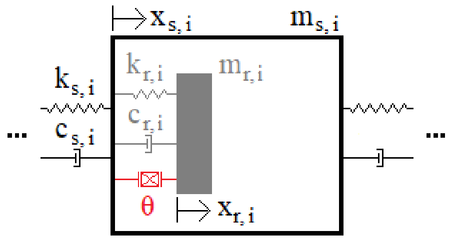

Figure 1 – Unit cell lumped model

$$m_{s,i}\ddot{x}_{s,i}(t)+c_{s,i}\left(\dot{x}_{s,i}(t)-\dot{x}_{s,i-1}(t)\right)+k_{s,i}\left(x_{s,i}(t)-x_{s,i-1}(t)\right)$$
$$+c_{r,i}\left(\dot{x}_{r,i}(t)-\dot{x}_{s,i}(t)\right)+k_{r,i}\left(x_{r,i}(t)-x_{s,i}(t)\right)-\theta v(t)-f_i(t)=0 \quad (1)$$

$$m_{r,i}\ddot{x}_{r,i}(t)+c_{r,i}\left(\dot{x}_{r,i}(t)-\dot{x}_{s,i}(t)\right)+k_{r,i}\left(x_{r,i}(t)-x_{s,i}(t)\right)+\theta v(t)=0 \quad (2)$$

Where *m*, *c* and *k* stands, respectively, for the mass, damp and stiffness of the system, θ is the electromechanic couple and *f* is the external force, the index *r* stands for the resonator cell and the *s* for the structure. Equations (1) and (2) are related to the actuator equation, Eq. (3), which describes the electric behavior of the system.

$$\frac{v(t)}{Z}+C_p\,\dot{v}(t)+\theta(x_{r,i}(t)-x_{s,i}(t))=0 \quad (3)$$

Equation (3) relates the mechanical displacement with the impedance, *Z*, and the internal capacitance of the piezo disk, C_p, when no external voltage source is considered, i.e., the direct piezoelectric effect is exploited.

For the mechanical modelling part, a clamped beam with flexural load is considered. Considering a homogeneous Euler-Bernoulli beam, one can write the potential energy for the continuous solution

$$U=\frac{1}{2}\int_0^L EI(w'')^2\,dx\,, \quad (4)$$

where the *EI* stands for the flexural stiffness of the Euler-Bernoulli beam, *L* is the total length. Also for kinetic energy, one can write

$$T=\frac{1}{2}\int_0^L \rho S(\dot{w})^2\,dx\,, \quad (5)$$

where *w* on the Eqs. (4) and (5) stands for the lateral displacement of the beam, which is variant in time and in position; *ρ* is the density of them beam material and *S* is the cross section area. As stated initially, a lumped model will be used. Thus, the finite form of Eqs. (4) and (5) with n elements as follows:

$$U = \frac{1}{2}\sum_{i=1}^{n}\frac{L}{n}EI\left(\frac{x_i - 2x_{i+1} + x_{i+2}}{\frac{L}{n}}\right)^2 , \tag{6}$$

$$T = \frac{1}{2}\sum_{i=1}^{n}\rho S\frac{L}{n}\dot{x}_i . \tag{7}$$

Therefore, the stiffness and mass matrix can be written, by using the Eqs. (6) and (7) to achieve the elementary parameters for a discrete beam as proposed by Eddanguir and Benamar (2013). Eventually, a space state representation of the system is evaluated with the addition of unit cell absorbers, in a progressive fashion as suggested in Fig. 2.

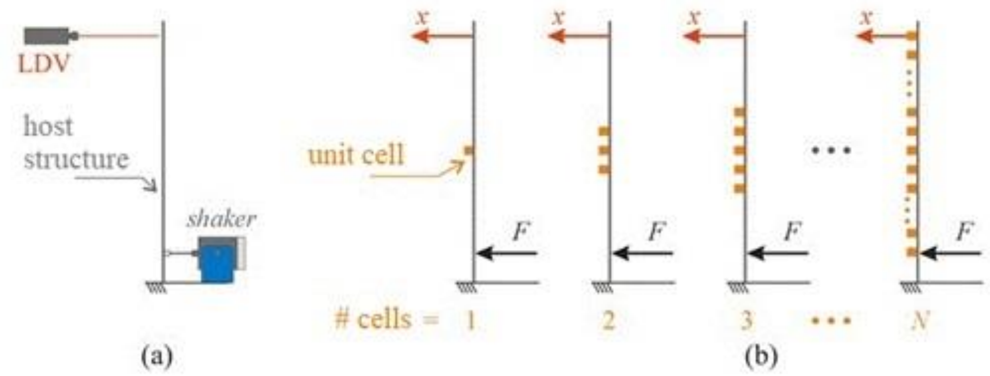

Figure 2 – concept for testing the smart metamaterial (a) host structure and (b) periodic array configuration with increasing number of unit cells

In addition, the modular modelling formulation presented by Rodrigues, da Silva and de Oliveira (2018) makes possible to evaluate a full smart metastructure embedded with piezo disks. Considerations about the unit cell model

As the proposed unit cell is a beam-like FDM printed part with piezo disks embedded, it is necessary to discuss some hypothesis around the model. Firstly, addressing the mechanical considerations, it is well known that most of FDM parts exhibits anisotropic behavior due to the manufacture process itself (Ahn et al., 2002). Even though, it is reasonable to assume planar isotropy for a layer working under traction-compression regime. Also, the layer shearing does not play a big role as consideration of Euler-Bernoulli beam so to speak. Also, the piezo disk suits this isotropic consideration. Therefore, it is possible to evaluate the mechanic structure as an ordinary isotropic material.

For this work, it is considered a lumped model with a single degree of freedom (DOF) for the modelling of the resonator, This consideration is based on the previous assumption of isotropic material, as the spring-mass system replicate the first vibrational mode. In addition, for better coherence of the mechanical response, it is considered a third tip mass, or active mass, with two thirds at the base, passive mass, that will be added to the host structure with the coupling, see Fig. 3. The density and stiffness proprieties of the ABS used on the FDM printing are validated by testing some printed beams and comparing the results against the output of a Finite Element Method model (Rodrigues, de Oliveira, da Silva, 2018).

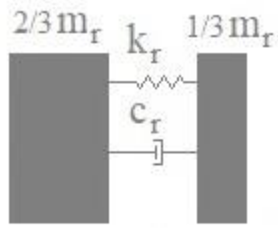

Figure 3 – Mechanical model of the unit cell

Also, it is important to keep track of the overall added mass to the structure as this is often a critical restriction on vibration absorbers. One can write the mass ratio as:

$$\mu = \frac{\sum_{i=1}^{n_r} m_r}{\sum_{i=1}^{n} m_s} \tag{8}$$

For the electric part, one can write for the internal capacitance of a piezo as:

$$C_p = e_{33} \frac{A}{h_p} \tag{9}$$

where e_{33} is a piezoelectric constant, a material propriety, A is the superficial area of the piezo, and h_p the height of the piezo, both geometric proprieties. Also the electromechanical coupling for bending load can be written as

$$\theta = e_{31} l_p d_n \tag{10}$$

where e_{31} is a piezoelectric constant, l_p is the piezo length, and d_n is the distance between the neutral axis of the substructure and the piezo for a unimorph beam.

Then, both proprieties are tied as they depend on physical dimensions. For the qualitative analysis presented on this work, will not focus on how to manipulate the dimensions to fit certain objectives, but by how the variation of those parameters influences the vibration suppression. Therefore, one can set a gain (A) to evaluate the performance as

$$C_p^A = C_p A_C \tag{11}$$

$$\theta^A = \theta A_\theta \tag{12}$$

where the superscript A denotes the modified propriety value. It is important to mention that afore a mentioned gain does not reflect a proportional control. Those gains should be interpreted as a geometrical variation of the piezoceramic and/or a change of material which leads to a change on the piezo constants. Then, a gain factor of 2 on the capacitance should be interpreted either as double the e_{33} or the superficial area or even cutting in half the thickness of the piezo, which in both cases are substantial variations.

For a start point, a piezo disk, see Fig. 4, will work as value reference for the piezoelectric parameters θ = 0.4774 mV/N and C_p = 18nF

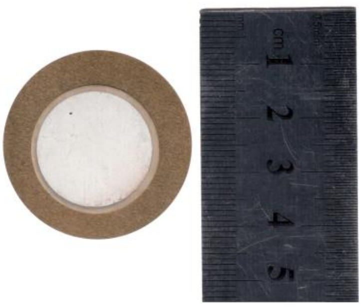

Figure 4 – Piezo disk capsule 35mm

RESULTS AND DISCUSSION

As discussed before, with the addition of multiple unit cell absorbers, the initial notch created by the first resonator evolves into a band gap, as can be seen in Fig. 5, which shows a color map of the transfer function between the shaker excitation and the tip response as the number of resonators increase. In this simulation, the total mass of the added metamaterial is kept the same, *i.e.*, the added mass is divided by whatever number of unit cells present in each configuration. The stiffness in those arrangements is also adjusted in order to maintain the targeted internal resonance frequency. It is possible to see that no improvement in band gap width or depth is obtained after the 10th cell, which configures the infinite convergence of the periodic metamaterial (Sugino et al., 2016b), Also, the appearance of two peaks on each side of the bandgap is clear from this plot. In this case, the lower frequency peak is the highest in amplitude, but the opposite can also happen. This is not an issue, when the disturbance excitation has a limited frequency band around the center of the bandgap, but could be a problem when broadband signal and/or variations in the disturbance frequency are expected and poses a challenge for the use of metamaterials in these cases.

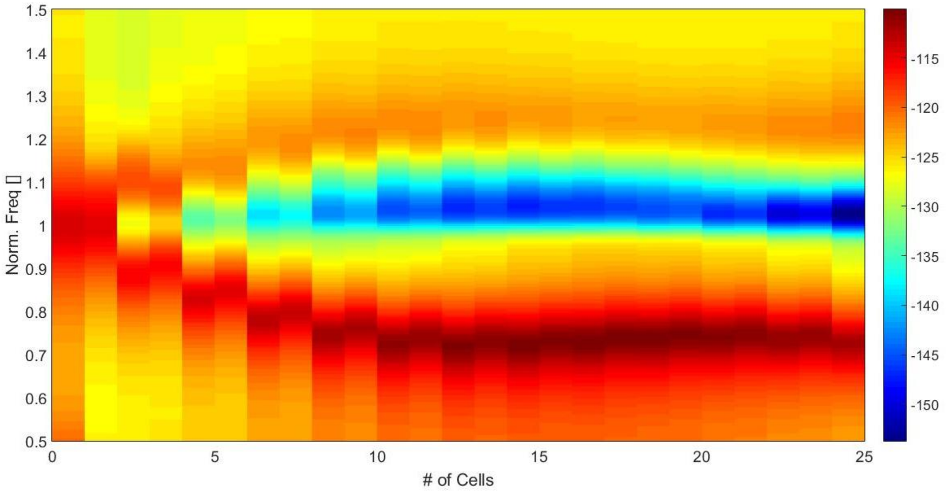

Figure 5 – Emergence of the band gap with increasing number of unit cells

In addition, the mass ratio influence is checked with the full convergence. As shown in Fig. 6, the increase in total added mass results in a performance gain as the band gap achieves a deeper and wider bandwidth ($\mu > 5\%$). In addition, after 25% it is possible to notice that the band gap width does not change significantly, as well as its depth, which penalizes the choices of heavier resonators. The upper peak created by the resonators also penalizes the higher mass resonators, as the peak goes from its higher frequency, around 10% ratio and 1.08 ω, back to the original frequency of the host structure, above 45% ratio.

A parabolic shape for the border peaks is noticeable. Inman (2008) presented a formulation for vibration suppression using a spring-mass resonator. However, it deviates from this result as his formulation does not take in account the added passive mass on the host structure with the coupling of the unit cell.

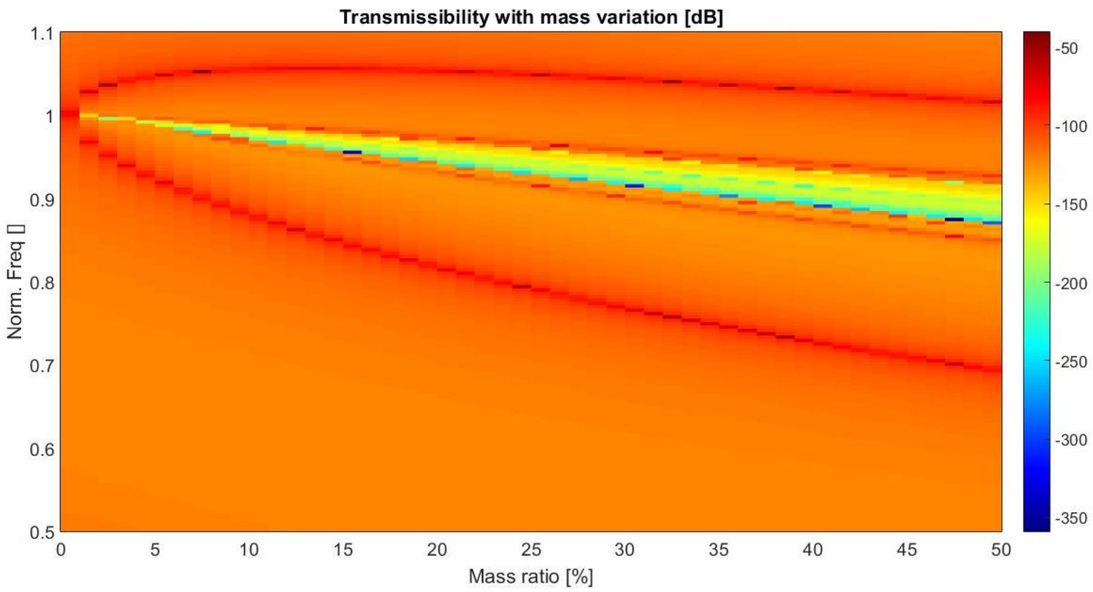

Figure 6 – Mass ratio influence on the host dynamic behaviour

In an attempt for achieving a wider bandgap width using smart metamaterials, this work proposes the tuning of the mechanical resonance for the main host resonance, while the electrical circuit is tuned for dealing with both upper and lower border peaks. The performance assessment and tuning of the electrical parameters is done via a series of sensitivity analyses using the electromechanical model. Firstly, dealing with the coupling factor itself for a simple unit cell with one mechanical DOF and a piezo for usage with a shunt LC type circuit, see Fig. 7.

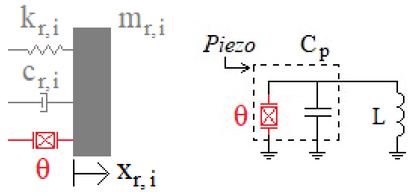

Figure 7 – Unit cell coupling arrangement

For this arrangement, an AB pattern is used, as both cells are mechanically tuned for the host resonance and the A cell works electrically on the lower frequency and the B cell on the higher. On Figure 8, it is possible to see the original structure behavior, going to a band gap with the addition of the unit cells. Then, with the contribution of the piezo shunt, both border peaks are reduced in around 20dB. With the increase of the A_θ value, both borders frequency peak are attenuated another 6dB more ($A_\theta = 0.9$), then disappear ($A_\theta > 1.2$), see Fig. 9. In addition to the borders suppression, some valleys appears on the gap zone leading to a wider gap at $A_\theta = 1.5$ as two valleys unites.

On the other hand, the increase of θ builds a peak around the 0.92 ω, as Fig. 9 shows, increasing in amplitude as A_θ increases. One can set an operational limit at $A_\theta = 1.8$, where the gap vanishes, and there is only a peak 10 dB lower than the original structure. Beyond this point, see Fig. 10, the increase of A_θ seems to nullify the mass penalty on the frequency, as the reminiscent peak walks back to the original peak, both in amplitude and frequency.

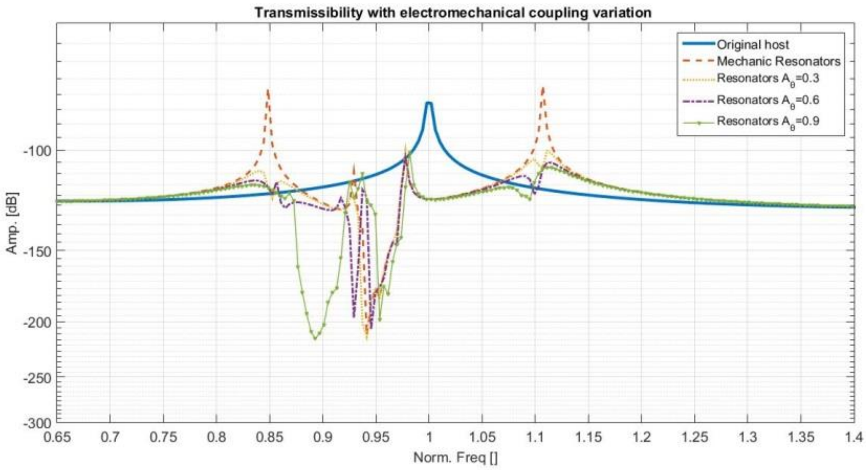

Figure 8 – Transmissibility with low electromechanical coupling

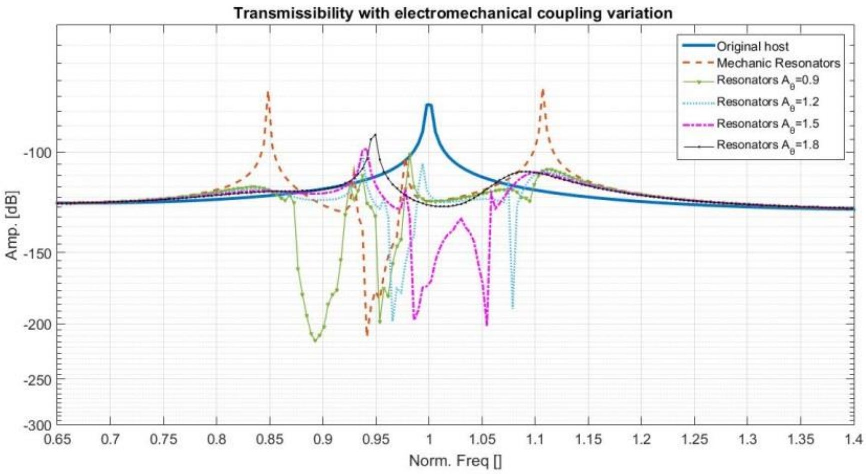

Figure 9 – Transmissibility with electromechanical coupling gain increasing up to 1.8

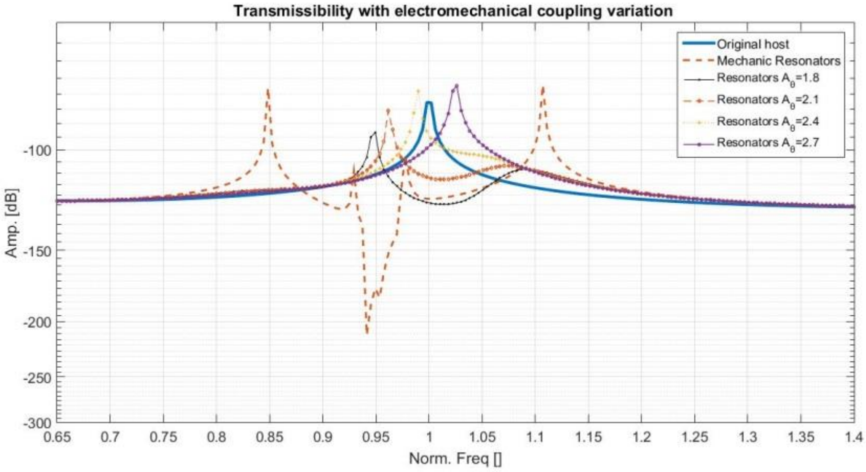

Figure 10 – Transmissibility with electromechanical coupling gain above 1.8

The internal capacitance analysis exhibits the inverse behavior of the coupling factor. As Figure 11 shows, a low capacitance leads to a very poor performance, analogous to a very high A_θ, and with the increase of the gain A_C a performance improvement is observed ($A_C > 1$), as multiple valleys emerge on the gap zone ($A_C > 1{,}5$), see Fig 12, and the border peaks remain around 30dB lower than the pure mechanic resonator, see Fig. 13.

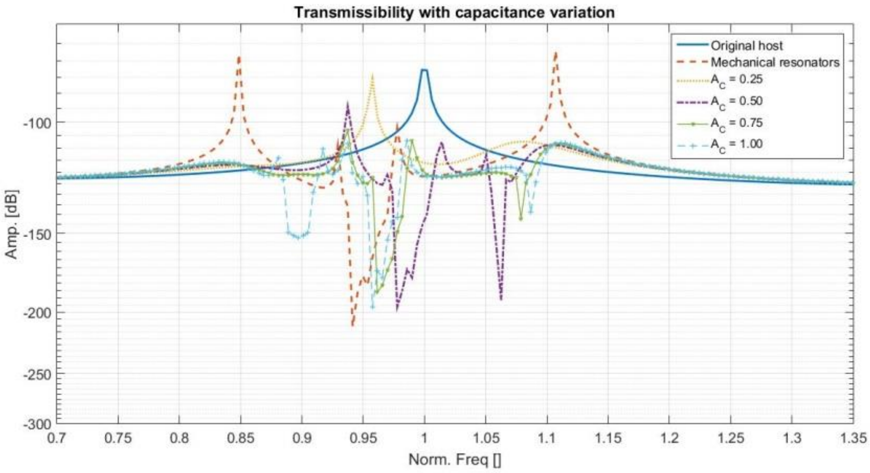

Figure 11 – Transmissibility with piezo capacitance variation from low to unity gain

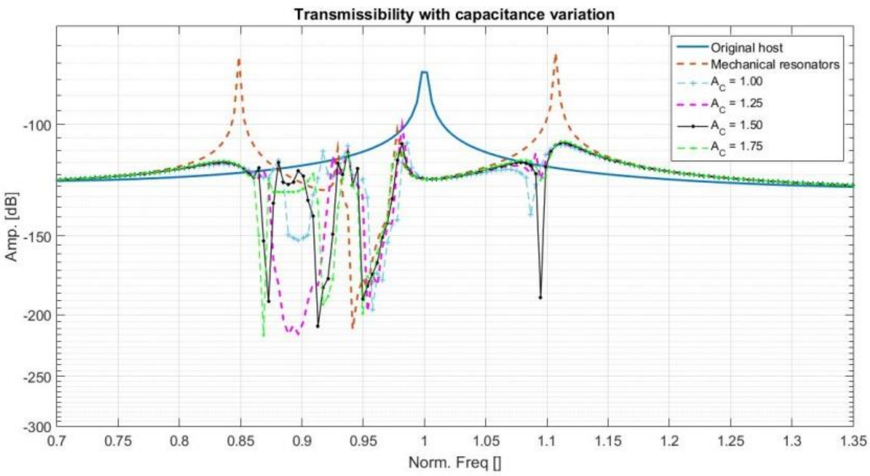

Figure 12 – Transmissibility with capacitance variation gain increasing up to 1.75

For the electrical manipulation, it is interesting a higher capacitance value, as the shunt relies on electrical resonance between an inductance and a capacitance. As the mechanical vibrations are often placed on a low frequency band, the higher capacitance lowers the required inductance value. Achieving high inductances is not an issue when dealing with synthetic inductors, but they introduce a big value of series resistance when compared to a passive inductor, especially in higher inductances.

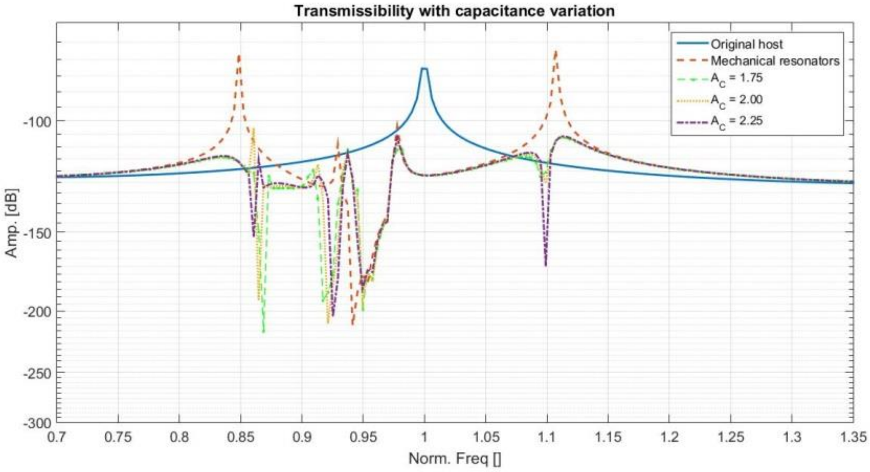

Figure 13 – Transmissibility with capacitance variation gain above 1.75

CONCLUSIONS

This work presents some insights for the smart metamaterial behavior as mechanical parameters for the beam transverse response with lumped resonators are modelled and some discussion about the FDM modelling hypothesis is addressed. In addition, the band gap convergence for infinite lattice is achieved with a finite number of cells and at the cost of border peaks around the gap. The mass ratio influence is also investigated suggesting a better cost benefit at $0.05 < \mu < 0.25$.

The border peaks were targeted as targets for the tuning of the electrical domain with passive circuitry. As results show, a small increment on the coupling factor leads to an increase in performance, but if the gain is set too high, it would lead to a very poor performance of the cell. Also, the internal capacitance influence was investigated, leading to an increase in performance for medium to high gains ($A_c > 1.5$).

As discussed before, the appearance of these peaks poses an interesting challenge for a new control approach that would target these peaks, instead of the central bandgap frequency, by the usage of the piezo disks combined with passive circuitry. The use of active control strategies for that matter is suggested as future work.

ACKNOWLEDGMENTS

The authors acknowledge the financial assistance of the Brazilian National Council for Scientific and Technological Development - CNPq (grant number 307369/2013-7) and the scholarship awarded to the first author also by CNPq.

REFERENCES

Ahn, S. H., Montero, M., Odell, D., Roundy, S., and Wright, P. K., 2002, “Anisotropic material properties of fused deposition modeling ABS”, Rapid Prototyping Journal, Vol. 8, No. 4, pp. 248–257.

Bilal, O. R., Foehr, A., and Daraio, C., 2017, “Observation of trampoline phenomena in 3D-printed metamaterial plates”, Extreme Mechanics Letters, Vol. 15, pp. 103–107.

Bosqué, C., 2015, “What are you printing? Ambivalent emancipation by 3D printing”, Rapid Prototyping Journal, Vol. 21, No. 5, pp. 572–581.

Claeys, C., Deckers, E., Pluymers, B., and Desmet, W., 2016, “A lightweight vibro-acoustic metamaterial demonstrator: Numerical and experimental investigation”, Mechanical Systems and Signal Processing, Vol. 70–71, pp. 853–880.

Cummer, S. A., Christensen, J., and Alù, A., 2016, “Controlling sound with acoustic metamaterials”, Nature Reviews Materials, Vol. 1, No. 3, p. 16001.

Eddanguir, A., and Benamar, R., 2013, “Transverses linear vibration of cantilever beam carrying two lumped masses . Analogy between discrete models”, 1st Euro-Mediterranean Conference on Structural Dynamics and Vibroacoustics, pp. 23–26.

Essink, B., and Inman, D. J., 2016, "A Comparison of Damping and Vibration Absorption in Metastructures", ISMA 2016 Proceedings, Leuven, Belgium, pp. 2025–2030

Hu, G., Tang, L., Banerjee, A., and Das, R., 2016, "Metastructure With Piezoelectric Element for Simultaneous Vibration Suppression and Energy Harvesting", Journal of Vibration and Acoustics, Vol. 139, No. 1, 11 p.

Huang, T.-Y., Shen, C., and Jing, Y., 2016, "Membrane- and plate-type acoustic metamaterials", The Journal of the Acoustical Society of America, Vol. 139, No. 6, pp. 3240–3250.

Inman, D. J., 2008, "Engineering vibration", Ed. Pearson Prentice Hall, Upper Saddle River, U.S.A, 669 p.

Li, F., Zhang, C., and Liu, C., 2017, "Active tuning of vibration and wave propagation in elastic beams with periodically placed piezoelectric actuator/sensor pairs", Journal of Sound and Vibration, Vol. 393, pp. 14–29.

Liu, Z., Zhang, X., Mao, Y., Zhu, Y. Y., Yang, Z., Chan, C. T., and Sheng, P., 2000, "Locally resonant sonic materials", Science (New York, N.Y.), Vol. 289, No. 5485, pp. 1734–1736.

Miranda Júnior, E. J. P., Ferreira, A. H. R., and dos Santos, J. M. C., 2017, "Flexural Wave Band Gaps In A Multi-Resonator Elastic Metamaterial Thin Plate", International Conference on Structural Engineering Dynamics ICEDyn 2017, 13 p.

Nouh, M. A., Aldraihem, O. J., and Baz, A., 2016, "Periodic metamaterial plates with smart tunable local resonators", Journal of Intelligent Material Systems and Structures, Vol. 27, No. 13, pp. 1829–1845.

Qureshi, A., Li, B., and Tan, K. T., 2016, "Numerical investigation of band gaps in 3D printed cantilever-in-mass metamaterials", Scientific Reports, Vol 6, p. 28314.

Raghavan, L., and Phani, A. S., 2013, "Local resonance bandgaps in periodic media: Theory and experiment", The Journal of the Acoustical Society of America, Vol. 134, No. 3, pp. 1950–1959.

Rodrigues, G. K., de Oliveira, L. P. R., and da Silva, M. M., 2018, "Modular modelling approach for FDM printed structures and piezo disks for metamaterial design", CILAMCE 2018 Proceedings, Paris/Compiègne, France.

Schumacher, C., Bickel, B., Rys, J., Marschner, S., Daraio, C., and Gross, M., 2015, "Microstructures to control elasticity in 3D printing", ACM Transactions on Graphics, Vol. 34, No. 4, pp. 136-150.

Sugino, C., Leadenham, S., Ruzzene, M., and Erturk, A., 2016, "On the mechanism of bandgap formation in locally resonant finite elastic metamaterials", Journal of Applied Physics, Vol. 120, No. 13, p. 134501

Sugino, C., Xia, Y., Leadenham, S., Ruzzene, M., and Erturk, A., 2016, "A General Theory for Bandgap Estimation in Locally Resonant Metastructures", Journal of Sound and Vibration, Vol. 406, pp. 104–123.

Yang, X. W., Lee, J. S., and Kim, Y. Y., 2016, "Effective mass density based topology optimization of locally resonant acoustic metamaterials for bandgap maximization", Journal of Sound and Vibration, Vol. 383, pp. 89–107.

Zhang, H., Wen, J., Xiao, Y., Wang, G., and Wen, X., 2015, "Sound transmission loss of metamaterial thin plates with periodic subwavelength arrays of shunted piezoelectric patches", Journal of Sound and Vibration, Vol. 343, pp. 104–120.

RESPONSIBILITY NOTICE

The authors are the only responsible for the printed material included in this paper.